Transition metals on the MgO(100) surface: Evolution of adsorption characteristics along the 4*d* series

Jacek Goniakowski
Centre de Recherche sur les Mécanismes de la Croissance Cristalline, CNRS, Campus de Luminy, Case 913, 13288 Marseille Cedex 9, France
(Received 16 October 1998)

We present a first-principles study of adsorption of 4*d* transition metals on the stoichiometric MgO (100) surface. We show that although the calculated evolution of adsorption energy along the series depends strongly on the adsorption site, the tendency of metal atoms to adsorb above the surface oxygen proves general. By analyzing the substrate-induced modifications of the electronic structure of the metal deposit we relate nonmonotonous evolution of adsorption energy found for this site to changes of cohesion of the deposited metal. [S0163-1829(99)09015-3]

I. INTRODUCTION

Growing technological interest in oxide-supported metal deposits has stimulated the theoretical effort to understand and efficiently model various metal-oxide interfaces.[1–4] The attention focuses principally on the growth and adhesion characteristics of the interface and on the substrate-induced properties of the electronic and atomic structure of the deposit. These factors are supposed to influence both directly and indirectly the reactivity and catalytic properties of metal deposits.[5] As a model substrate, the MgO (100) surface is probably the most widely used for both experimental and theoretical studies.[6] On the one hand, experimentally it is relatively easy to obtain a clean, well-characterized MgO (100) facets of small defect density and well-defined stoichiometry.[7] On the other hand, simplicity of MgO's cubic structure and the reported lack of strong structural modifications upon metal deposition reduce the computational effort of numerical modelling. At the same time, since MgO is a wide gap insulator of a strong ionic character, it is an excellent model substrate for studies on nonreactive interfaces, for which the adhesion is attributed mainly to image charge and van der Waals interactions without any significant chemical hybridization and charge transfer.[8] In fact, for the metal/oxide interfaces, the relative importance of different energetic contributions to the adhesion is rather poorly known and at present their description is based principally on the empirical grounds. Furthermore, since the systems studied experimentally are relatively complex and a direct verification of the theoretical results as to validate the proposed models is often not possible, many fundamental questions on the adequacy of modelling tools remain open.[4,9–11]

It is only very recently that studies founded on *ab initio* electronic band-structure calculations devoted to deposition of chosen transition metals, principally from the end of the transition series, were reported.[8,12–19] Satisfactory agreement with experimental results on the basic interface characteristics (the preferential adsorption site, interface separation, adhesion energy) proves that the state of art electronic band-structure approaches are likely to be adequate for description of metal-oxide systems. However, the fundamental microscopic mechanisms responsible for the cohesion and structure of the interface are still far from being fully understood, and any unified picture of the metal-oxide interactions has not yet emerged.[4,20] This is also the case of the understanding of substrate-induced modifications of the electronic characteristics of deposited metal and of their relation to the deposit's reactivity.

It is the goal of this paper to add new elements to the most fundamental understanding of the processes on the metal-oxide interface. To this aim, we have undertaken a systematic study of the 4*d* transition-metal deposition on the MgO (100) surface. Although some of the considered systems do not present any direct experimental interest, altogether they give a coherent picture of the evolution of the interface characteristics in function of the properties of deposited metal and give a systematic view on factors that influence the metal-oxide bonding. Following this strategy and wanting to consider all the metals on the same footing, we have chosen the simplest, epitaxial monolayer deposit geometry. Although for some of the considered metals it does not correspond to the experimentally reported growth mode, it has the advantage of giving a direct access to the information on interface-formation-induced modifications of the electronic structure and of making the analysis of evolution of bonding characteristics along the series relevant. For the same reasons in the present paper we have neglected the magnetic effects, considering all systems as paramagnetic. In this way, although not directly applicable to the interpretation of existing experiments, the present study constitutes a base for a future modelling of more complex systems.

The paper is organized as follows. In Sec. II we briefly describe the method used for the electronic structure calculations. In Secs. III and IV, respectively, we present and discuss obtained results. We conclude in Sec. V.

II. TECHNIQUES

For the present paper we have used the local-density approximation (LDA)-based, full potential linearized muffin-tin orbitals (FP-LMTO) method,[21,22] which has already proven it's adequacy for systems of both metallic and insulating character. Additionally, no shape approximation on the

Khon-Sham potential and on the electronic density makes it also suitable for systems of lower symmetry, like surfaces and interfaces.[23–25] In particular, this method has been already successfully used in studies on metal/oxide interfaces and on deposition of transition metals on oxides.[12,19] Additionally, by the gradient-corrected linear augmented plane-wave approach,[26] we have verified that the evolution of adsorption characteristics presented in the following sections is not influenced by the employed approximations.

Within the FP-LMTO method space is divided into non-overlapping spheres centered on the atomic sites. Spheres of 1.91 a.u. were used for oxygen and magnesium atoms and of 2.45 a.u. systematically for all the transition-metal atoms considered. The basis set consists of atom-centered Hankel envelope functions, which are augmented inside the atomic spheres by means of a numerical solution of the scalar-relativistic Dirac equation. Due to the non-vanishing interstitial region it is enough to use a minimal basis set: we have used three s, three p, and three d functions per atomic site at three different energies (-0.7, -1.0, and -2.3 Ry), corresponding to three different localizations of Hankel envelopes.[12] Valence states are O($3s2p3d$), Mg($3s3p3d$), and ($4d5s5p$) for the transition-metal atoms. Furthermore, we have used the two-panel technique in order to include the $2s$ electrons of oxygen, $2p$ electrons of magnesium, and $4p$ semicore electrons of transition metal as full band states. In order to obtain an accurate representation of the decaying electronic density outside the surface it is often necessary to increase the basis set by filling the interstitial region with empty spheres. In the present calculations we have included the empty spheres that are first neighbors of the deposited monolayer atoms. The space between the oxygen and magnesium atoms inside the slab and at the interface was also filled with empty spheres.[12]

Results of convergence tests performed on the Pd/MgO system as well as on the separated Pd and MgO bulk and surfaces are described in more detail in Ref. 19. For the present paper we have adopted the same computational settings: an unrelaxed, five-layer-thick MgO slab (of bulk MgO lattice parameter), two-dimensional k-point sampling with 6 k points in the irreducible part of the two-dimensional (2D) Brillouin zone (with a 20 mRy Gaussian broadening for the calculation of the density of states). In order to compensate possible lack of full convergence, all calculations (free MgO surface, unsupported and deposited metal layers) were performed in exactly the same periodic cell.

III. RESULTS

In the following we will present the principal results of the electronic structure calculations on deposition of 4d metal monolayer on the MgO (100) surface starting by the results on evolution of adsorption energy along the transition series and on its relation to the adsorption site. Next we report the results on the adsorption-induced modifications of the electronic structure of the substrate and of the deposited monolayer. In Sec. IV we analyze the results and focus on the relation between the electronic structure and the energetics.

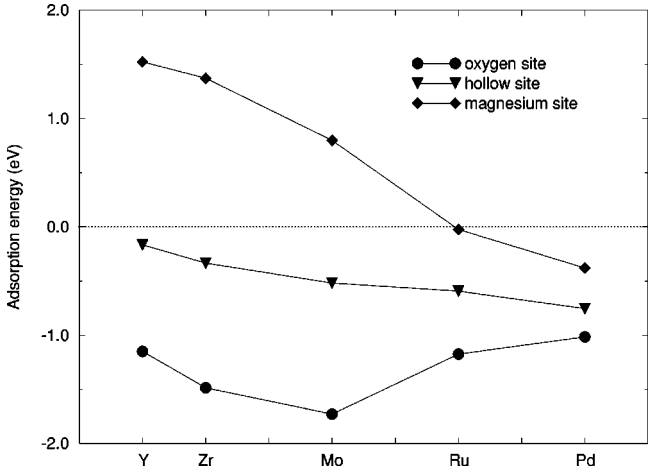

FIG. 1. The adsorption energy calculated for 4d transition-metal monolayers deposited on the MgO (100) surface. Three alternative adsorption geometries are depicted: metal atom above a surface oxygen, above a surface magnesium, and in a surface hollow site.

A. Adsorption energetics

In Fig. 1, we present the calculated evolution of the adsorption energy along the 4d transition series. Three inequivalent adsorption geometries were considered: metal atoms above surface oxygens, above surface magnesiums, and in the surface hollow sites (in between surface ions). In order to better access the tendencies of interest for the present study, for all the considered systems, adsorption energy was calculated for a fixed distance between the deposited metal layer and the MgO surface (2.37 Å). We have verified, however, that the optimization of the interfacial spacing influences only slightly the reported values and that it does not modify at all the character of their evolution along the series. On the other hand, since our goal is to analyze the metal-oxide bonding, by representing the adsorption energy with respect to an unsupported metal monolayer strained as to match the MgO's lattice parameter (rather than representing it with respect to free metal atoms), we have eliminated the contribution due to the formation of the horizontal metal-metal bonds (which would otherwise dominate the adsorption energetics). The adsorption energy being calculated as a difference of total energies, its more negative value corresponds to a stronger adsorption.

All considered metal monolayers show a well-pronounced preference to adsorb above the surface oxygen, magnesium site being in all cases energetically the most unfavorable. This tendency, which was already reported on the theoretical grounds for adsorption of chosen 3d and 4d metals of the end of the transition series, proves thus to be systematic. Experimentally, palladium atoms were seen above surface ions,[27] and palladium and silver atoms were seen above surface oxygens.[28] The evolution of the adsorption energy along the series shows a qualitatively different character for the free different adsorption sites. For the less energetically favorable sites (the cation and the hollow one) it decreases monotonously from the beginning to the end of the series. This decrease is rapid for adsorption above the surface cation, whereas the adsorption energy calculated for the hollow site varies little as a function of the deposited metal. On the contrary, for the oxygen site, the dependence is nonmonoto-

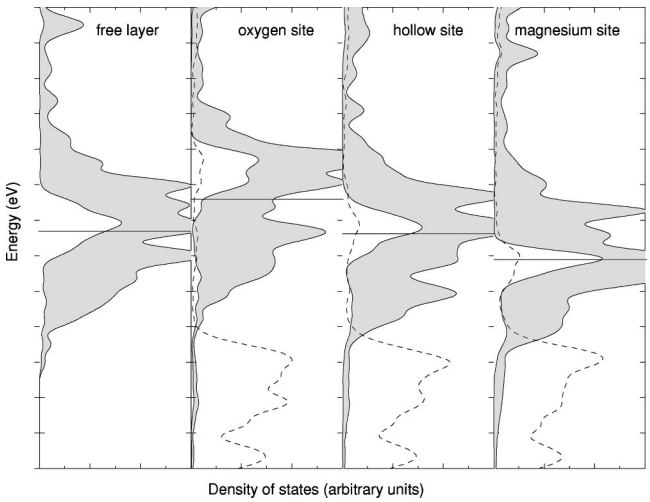

FIG. 2. Layer-projected DOS calculated for an unsupported (strained) Mo monolayer and for the same monolayer deposited on the MgO (100) surface in three alternative adsorption geometries. Projection on the $d_{3z^2-r^2}$ orbital is plotted explicitly. Dashed lines represent surface projected DOS of the substrate.

nous and shows a well-pronounced minimum (corresponding to the maximal bonding strength) for metals from the middle of the series.

This untypical nonmonotonous behavior substantially differs from the results of semi-empirical calculations of 3*d* metal deposition on Al_2O_3, where a monotonous weakening of the adsorption energy along the series was reported.[29] Results obtained recently by Yudanov *et al.*[15] concerning the adsorption of isolated metal atoms from the second half of the transition series show also a progressive weakening of the adsorption energy. However, very recent *ab initio* calculations of adsorption energy of transition metals from the 5*d* series on the TiO_2 (110) surface seem to show a similar, nonmonotonous evolution.[30]

B. Electronic structure: Influence of the adsorption site

Since the difference of adsorption energies obtained for different adsorption sites is the most pronounced for adsorption of molybdenum, we have chosen this case to visualize the site-dependence of the modifications of the deposit's electronic structure. In Fig. 2, we present the density of states (DOS) calculated for an unsupported, strained molybdenum monolayer, and for the same monolayer deposited in the three alternative adsorption geometries. Projection was made on the atomic spheres of surface atoms and on the sphere of molybdenum. Additionally the $d_{3z^2-r^2}$ component of the molybdenum DOS is plotted explicitly (z-axis points in the [001] direction). The energy scales were shifted as to align the DOS projected on the atoms in the center of the slab (not shown in the figure).

Two principal points are to be underlined. The position of the valence band of the deposited metal relative to the valence band of MgO changes in function of the adsorption site. This global shift of the metal band has been already reported for palladium deposited on the MgO (100) and attributed to the monopole contribution of the substrate electrostatic field.[19] This latter is repulsive above the surface anions (an upward shift of adsorbate atomic levels), attractive above the surface cations (a downward shift of adsorbate levels), and close to zero for the surface hollow site. The evolution of the molybdenum DOS depicted in Fig. 2 matches well this scheme. On the other hand, it is to be seen that the adsorption-induced modifications of the metal valence band go beyond the described rigid shift, and concern also the fine structure of the metal DOS. With respect to its position in the *d* band of the unsupported monolayer, the $d_{3z^2-r^2}$ orbital is shifted upwards when deposited above the surface anion, downwards when deposited above the surface cation, whereas its position is only little modified when deposited in the surface hollow site. As already pointed out in Ref. 19 this additional splitting of the *d* band of the adsorbate can be related to the crystalline-field-like coupling between the symmetry of different *d* components and this of the substrate electrostatic field.

At the same time, for all three considered geometries, Fig. 2 gives the evidence of hybridization between the orbitals of the deposited metal monolayer and those of surface oxygens. On the one hand an additional peak, corresponding to bonding metal-oxygen states, splits off from the top of the substrate valence band. It is the most pronounced in the case of metal deposited above the surface oxygen, whereas its intensity is small for deposition above the surface magnesium. On the other hand, the hybridization between the oxygen and molybdenum states shows the location of the antibonding metal-oxygen contribution in the metal-projected DOS. It is important to notice that the position of the antibonding states relative to the Fermi level changes dramatically as a function of the deposition geometry. When adsorbed above the surface anion, the major part of the antibonding states is unoccupied. In the opposite limit, when adsorbed above the cation the antibonding states are to a considerable extent below the Fermi level.

C. Electronic structure: Evolution along the series

In the present section, we will focus on the evolution of the interface electronic structure along the transitions series. We have chosen to focus the attention on two adsorption geometries presenting opposite adsorption characteristics, namely on adsorption above the surface anion or above the surface cation. In Fig. 3, we present corresponding DOS projected on the atomic spheres of surface atoms and of adsorbed metal. Again, the $d_{3z^2-r^2}$ component of metal *d* band is plotted explicitly. The energy scales are aligned as to match the DOS projected on the substrate atoms in the center of the slab (not shown in the figure).

The principal characteristics of the evolution of the metal band along the series correspond to those of a free-metal layer and are determined mainly by the increasing atomic number. Thus, from left to right of the series we find a successive reduction of the width of the metal band coupled to its progressive overall shift towards lower energies. At the same time, the number of electrons in the metal band increases. The character of the adsorption-induced modifications of the metal band, shows the features that have already been pointed out in the preceding section. On the one hand, when deposited above a surface cation, the metal band is about 1 eV higher (with respect to the top of the substrate valence band) than when deposited above a surface cation. On the other hand, changes of its form are in all cases domi-

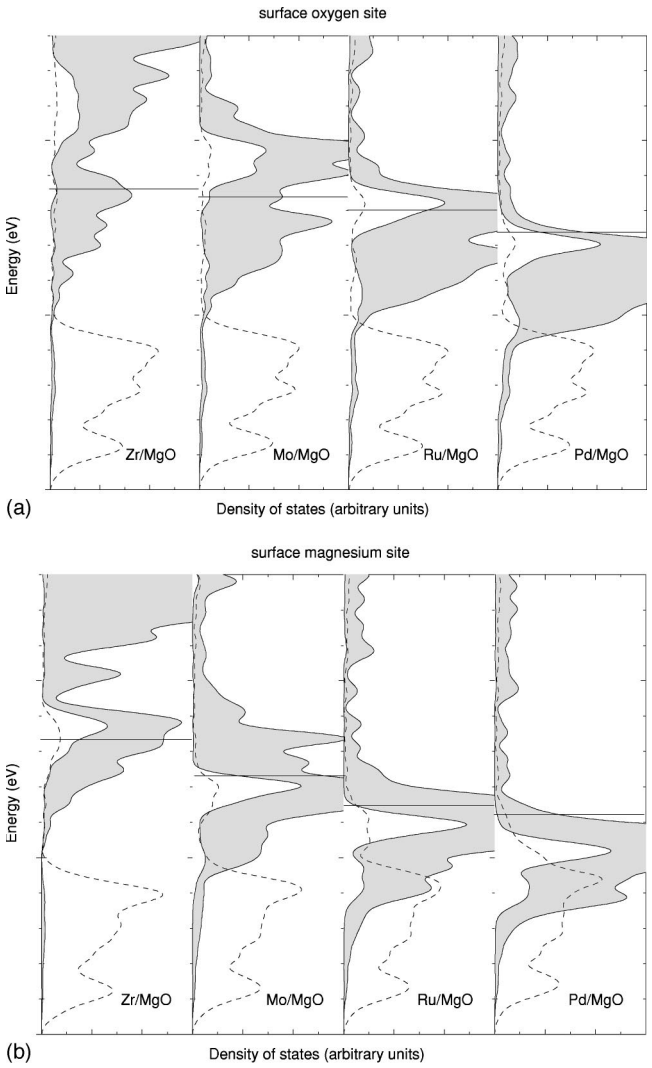

FIG. 3. Layer-projected DOS calculated for 4*d* transition-metal monolayers deposited on the MgO (100) surface: (a) metal atoms above a surface oxygen, and (b) above a surface magnesium. Projection on the $d_{3z^2-r^2}$ orbital is plotted explicitly. Dashed lines represent surface projected DOS of the substrate.

nated by the relative shift of the $d_{3z^2-r^2}$ component with respect to the *d* band center of gravity. Systematically, the $d_{3z^2-r^2}$ component of the metal DOS is pushed upwards when adsorbed above the surface oxygen and downwards when adsorbed above the surface cation.

Let us now focus on the signature of the metal-oxygen bonding for the energetically favorable configurations (adsorption above surface anions). Substrate's DOS in the region of the metal band reveals the location of the antibonding states, which in all the cases coincides with the $d_{3z^2-r^2}$ peak. Along the series, due to the increasing number of electrons in the metal band, the antibonding states become progressively filled. The substrate-projected DOS is very similar for all the considered systems. With respect to a clean MgO surface, an additional peak in the substrate valence band is to be seen. Due to its mixed character it can be attributed to the bonding oxygen-metal states. Across the series, its position with respect to the substrate band remains roughly constant, whereas its intensity increases.

IV. DISCUSSION

Although for most of the considered systems any direct comparison with the experiments is not possible, present computational results show several very clear tendencies that can shed a new light on the understanding of the electronic structure and of the cohesion of metal-oxide interfaces. Since the monotonous character of the evolution of adsorption energy for metal deposited over the surface cation can be regarded as controlled principally by the repulsion between the metal atom and the surface cation, it thus reflects the decrease of metal atomic radii along the series. In the following we will focus our attention on the nonmonotonous evolution of the adsorption energy for metal adsorbed in the energetically favorable geometry, namely above the surface anions.

As it was already pointed out, Fig. 3 reveals the existence of covalent bonds between the deposited metal atoms and the surface anions. Although the separation between the oxygen and metal atomic levels decreases along the series, the position of the bonding metal-oxygen states with respect to the substrate valence band does not change significantly. In a simple molecular-orbital diatomic diagram this can be explained as due the compensation between the simultaneous decrease of the atomic-level separation and of the metal-oxygen hopping integrals (the latter being related to the decreasing atomic radii of metal). Within this picture the intensity of the oxygen contribution to the bonding states changes with a square of the atomic level separation and so, as it can be seen in Fig. 3, it increases along the series. On the other hand, form left to right of the series, the antibonding states get progressively filled, resulting in a monotonous decrease of the metal-oxygen bond strength. This simple picture has been already used in the study on the deposition of the 3*d* transition metals on Al_2O_3,[29] where authors hold it responsible for the calculated, monotonous weakening of the adsorption energy along the series.

However, present results reveal a qualitatively different character of the evolution of adsorption energy, suggesting that although present, this is not the direct oxygen-metal bonding that dominates the overall energetic characteristics. Similar energetics, obtained for 5*d* transition metals deposited on the TiO_2 (100) surface has been interpreted in terms of the deposition-induced charge redistribution within the substrate.[30] In the case of MgO however, its strongly pronounced ionic character attenuates any charge redistribution within the substrate. In fact, existing results show an absence of any important charge transfer between the substrate and the metal deposit or charge redistribution in the substrate.[12,19] At the same time however, the interaction of metal deposit with the surface electrostatic field becomes more important, which in absence of charge transfer across the interface provokes principally a redistribution of electrons between different *d* components in the valence band of the monolayer. From Fig. 2 it is clear that when deposited above oxygen the $d_{3z^2-r^2}$ orbital transfers its electrons to the rest of the *d* band, the opposite being true for adsorption above the cation. Inspection of Fig. 3 shows that this scheme persists along all the series.

In the simple tight-binding approach, the cohesion of the metal monolayer is determined by the filling of its *d* band. Along the transition series, the progressive filling of the

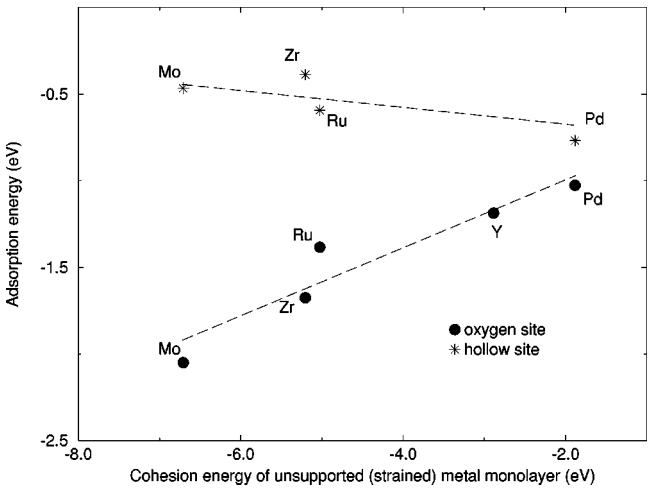

FIG. 4. Calculated evolution of adsorption energy as a function of the cohesion energy of the unsupported (strained) monolayer for the 4*d* transition metals. Dashed lines are plotted as a guide for the eye.

bonding, then antibonding states explains the well-known parabolic character of evolution of the cohesion energy. In the case of an unsupported monolayer, different *d* components contribute differently to its cohesion. In particular, the $d_{3z^2-r^2}$ components overlap little, their contribution is thus small. Changing their electronic population modifies only little the cohesion energy, if compared to the effect of population changes in the rest of the *d* band. Thus, the substrate-induced upward shift of the metal $d_{3z^2-r^2}$ component and related transfer of electrons from this component to the rest of the *d* band modifies the cohesion of the deposit, the change being proportional to the cohesion energy. In Fig. 4, we have plotted the adsorption energy of the metal layer deposited above the surface oxygen or in the surface hollow site as a function of the cohesion energy of the unsupported (strained) layer. In fact, it is to be seen that whereas for the hollow site, the adsorption energy changes little along the series (cf Fig. 1), for the oxygen site it changes proportionally to the changes of the cohesion energy of the free layer.

Figure 4 gives also an estimate of the height of the static diffusion barrier for a collective migration of the metal atoms over the MgO (100) surface. This diffusion barrier can be calculated as an energy difference between the minimum (above the oxygen site) and the saddle point (above the hollow site) of the adsorption energy surface. We find that for metals from the middle of the series (strong adsorption energy) the barrier is maximal, and it decreases towards both ends of the series (small adsorption energies). This further proportionality between adsorption energy and the height of diffusion barrier correlates well with tendencies deduced from the experimental results.[31]

V. CONCLUSIONS

Our first-principles calculations of the deposition of the 4 *d* transition metals on the stoichiometric MgO (100) surface show that the tendency of metal atom to favor adsorption above the surface oxygen, which was already reported for chosen metals from the end of the series proves to be more general. We have shown that whereas the adsorption energy calculated for adsorption above the surface magnesium or in the surface hollow site vary monotonously along the series, the evolution of the adsorption energy for adsorption above the surface oxygen displays a parabolic character with the maximal adsorption strength for metals from the middle of the series. When discussing the adsorption-induced modification of the electronic structure of the interface, we have emphasized the importance of the substrate-field-induced polarization of the deposit and on related changes of its cohesion.

ACKNOWLEDGMENTS

We thank C. Noguera, C. Henry, and G. Tréglia for their interest and stimulating discussions. The major calculations were performed on the CRAY C98 computer at IDRIS, under Project No. 960732. We are grateful for a generous allocation of time on the machine. The CRMC^2 is also associated with the Universities of Aix-Marseille II and III.

[1] C. Noguera, *Physics and Chemistry at Oxide Surfaces* (Cambridge University Press, Cambridge, 1995).
[2] G. Bordier and C. Noguera, Phys. Rev. B **44**, 6361 (1991).
[3] F. Didier and J. Jupille, Surf. Sci. **314**, 378 (1994).
[4] M. W. Finnis, J. Phys.: Condens. Matter **8**, 5811 (1996).
[5] *Chemisorption and Reactivity on Supported Clusters and Thin Films*, edited by R. M. Lambert and G. Pacchioni (Kluwer Academic, Dordrecht, 1997).
[6] V. E. Henrich and P. A. Cox, *The Surface Science of Metal Oxides* (Cambridge University Press, Cambridge, 1994).
[7] C. Duriez, C. Chapon, C. R. Henry, and J. Rickard, Surf. Sci. **230**, 123 (1990).
[8] C. Li, R-q. Wu, A. J. Freeman, and C. L. Fu, Phys. Rev. B **48**, 8317 (1993).
[9] G. Bordier and C. Noguera, Phys. Rev. B **44**, 6361 (1991).
[10] M. W. Finnis, Acta Metall. Mater. **40**, S25 (1992).
[11] See, e.g., J. R. Smith, T. Hong, and D. J. Srolovitz, Phys. Rev. Lett. **72**, 4021 (1994), followed by M. W. Finnis, R. J. Needs, and U. Schönberger, *ibid.* **74**, 3083 (1995).
[12] U. Schönberger, O. K. Andersen, and M. Methfessel, Acta Metall. Mater. **40**, S1 (1992).
[13] R-q. Wu and A. J. Freeman, Phys. Rev. B **51**, 5408 (1995).
[14] A. M. Ferrari and G. Pacchioni, J. Phys. Chem. **100**, 9032 (1996).
[15] I. V. Yudanov, G. Pacchioni, K. Neyman, and N. Rösch, J. Phys. Chem. B **101**, 2786 (1997).
[16] K. Neyman, S. Vent, G. Pacchioni, and N. Rösch, Nuovo Cimento D **19**, 1743 (1997).
[17] A. Stirling, I. Gunji, A. Endou, Y. Oumi, M. Kubo, and A. Miyamoto, J. Chem. Soc., Faraday Trans. **93**, 1175 (1997).
[18] V. Musolino, A. Selloni, and R. Car, J. Chem. Phys. **108**, 5044 (1998).
[19] J. Goniakowski, Phys. Rev. B **57**, 1935 (1998); **58**, 1189 (1998).
[20] G. Pacchioni and N. Rösch, J. Chem. Phys. **104**, 7329 (1996).
[21] M. Methfessel, Phys. Rev. B **38**, 1537 (1988).

[22] M. Methfessel, C. O. Rodriguez, and O. K. Andersen, Phys. Rev. B **40**, 2009 (1989).
[23] M. Methfessel, D. Hennig, and M. Scheffler, Phys. Rev. B **46**, 4816 (1992).
[24] J. N. Andersen, D. Hennig, E. Lundgren, M. Methfessel, R. Nyholm, and M. Scheffler, Phys. Rev. B **50**, 17 525 (1994).
[25] S. Sawaya, J. Goniakowski, C. Mottet, A. Saúl, and G. Tréglia, Phys. Rev. B **56**, 12 161 (1997).
[26] P. Blaha, K. Schwarz, and J. Luitz, WIEN97 (Vienna University of Technology, Vienna, 1997). [Improved and updated Unix version of the original copyrighted WIEN code, which was published by P. Blaha, K. Schwarz, P. Sorantin, and S. B. Trickey, Comput. Phys. Commun. **59**, 399 (1990).]
[27] S. Giorgio, C. Chapon, C. R. Henry, and G. Nihoul, Philos. Mag. B **67**, 773 (1993).
[28] G. Renaud Surf. Sci. Rep. **32**, 1 (1998).
[29] K. Nath and A. B. Anderson, Phys. Rev. B **39**, 1013 (1989).
[30] L. Thiên-Nga and A. T. Paxton (unpublished).
[31] J. A. Venables, G. D. T. Spiller, and M. Hanbücken, Rep. Prog. Phys. **47**, 399 (1994).